Title Page (with Author Details)

Feasibility of realizing daytime solar heating and radiative cooling simultaneously with a novel structure

Mingke Hu [a], Bin Zhao [b], Suhendri [a], Jingyu Cao [c], Qiliang Wang [d], Saffa Riffat [a], Yuehong Su [a, *], Gang Pei [b, *]

[a] *Department of Architecture and Built Environment, University of Nottingham, University Park, Nottingham NG7 2RD, UK*

[b] *Department of Thermal Science and Energy Engineering, University of Science and Technology of China, Hefei 230027, China*

[c] *College of Civil Engineering, Hunan University, Changsha 410082, China*

[d] *Department of Building Services Engineering, The Hong Kong Polytechnic University, Kowloon, Hong Kong, China*

---

* Corresponding author: yuehong.su@nottingham.ac.uk; peigang@ustc.edu.cn

Feasibility of realizing daytime solar heating and radiative cooling simultaneously with a novel structure

Abstract

Recent breakthroughs in preparing near-perfect emitters have made it possible to realize daytime radiative cooling under intensive solar radiation. However, a typical radiative cooler cannot deliver heat and may even cause an undesired cooling effect on cold days. Instead of rejecting the solar radiation back to the sky, this work proposes a new concept of capturing this “free” renewable energy while dumping waste heat through radiative cooling. The new structure features an upper solar-transparent radiative emitter and a lower solar absorber. Simulation results suggest that, to realize daytime solar heating and radiative cooling simultaneously, the emitter solar-absorptivity should be extremely low, and the absorbed solar heat should be instantly and effectively taken away by thermal carriers. With an ambient temperature of 25 °C and a maximum solar irradiance of 1000 W/m^2, the emitter can always reach a sub-ambient temperature if the absorber temperature is lower than 33.9 °C in the non-vacuum case, and can exceed 70 °C if the air cavity between the emitter and absorber is vacuumized. A performance simulation in three consecutive days in Shanghai reveals that the emitter can realize daytime radiative cooling with a temperature reduction of over 9.3 °C from the ambient temperature around noon.

Keywords: *solar energy; solar heating; radiative cooling; simultaneously; vacuum*

1. Introduction

Heating and cooling are essential in modern society but are responsible for huge fossil energy consumption and serious environmental pollution [1, 2]. Therefore, developing renewable and environmental-friendly technologies to deliver thermal energy is increasingly imperative. The sun (~5800 K) and deep universe (~3 K) are respectively the ultimate renewable heat and cold sources for the earth [3]. Therefore, solar heating and radiative cooling are two appealing solutions to achieve decarbonization [4, 5].

Solar heating (hereafter referred to as the 'SH') is one of the dominant solar energy technologies, converting most incident solar radiation into heat using a solar thermal collector [6, 7]. After several decades of development, SH has become a commercial technology that widely applies in buildings [8], industry [9], and agriculture [10], etc. In contrast, radiative cooling (hereafter referred to as the 'RC') did not receive much attention until the last decade, though it is an anciently discovered natural phenomenon [11]. RC provide an appealing strategy to mitigate global warming as it sends waste heat to the outer space without driving power [12-14]. RC has shown great potential in building energy-saving [15] and personal thermal management [16]. Subjected to the difficulty of fabricating a spectrally near-perfect RC emitter, this passive cooling technology has been long limited to only night-time operation [17, 18]. However, with the breakthroughs in materials science, RC under intensive solar radiation was successfully realized by Raman et al. in 2014 [19]. Since then, daytime RC has experienced booming developments, with the manufacturing of a near-ideal emitter heading towards much more accessible, cheaper, and more scalable approaches [20, 21].

However, as most of the available RC emitters are spectrally-static, they may produce unwanted coldness on cold days. Though spectrally-adaptive emitters that can “turn off” the RC function on cold days have been proposed recently [22, 23], they are unable to effectively harness solar heat due to insufficient solar absorption. Therefore, an RC device may be out of operation for a long period throughout a year in four-season regions. This intermittent working nature, coupled with relatively low cooling power density compared to the mainstream vapor compressing refrigeration [24], leads to poor practicability of the stand-along RC device. Similarly, a stand-alone SH collector shows low emissivity excluding the solar radiation band, especially within the “atmospheric window”, making it of little value in hot seasons and cannot work at night [25].

We previously proposed a dual-functional solar heating and radiative cooling (SHRC) collector equipped with a spectrally-coupled panel to conduct SH during the daytime and act as an RC device during the nighttime [26]. The spectrally coupled panel showed high absorptivity and emissivity in the solar radiation band and “atmospheric window”, but relatively low in the rest bands. The collector radiatively lost an amount of heat in solar heating mode due to the high emissivity in the “atmospheric window”, and thus its SH efficiency was about 80% that of a conventional SH collector. Moreover, although cooling loads usually dominate during the daytime, especially during the peak sun hours, this spectrally-coupled SHRC collector can never provide coldness at daytime due to its high solar absorptivity, which affects its practicability on hot days. It would be attractive if a collector can simultaneously harvest solar heat and universe coldness during the daytime, fully harnessing the two renewables from the out space. Zhai et al. [27] delivered a transparent RC film which shows very high long-wave emissivity but extremely high solar transmissivity before being backed with a silver coating. The silver coating helps to reflect about 96% of solar radiation back to

the sky. This structure inspires us that, instead of rejecting this free but valuable solar energy, we can capture and utilize it by setting a solar absorber below the transparent RC film. Such a modification may enable the collector to simultaneously deliver heat and coldness during the daytime, thus enhancing the renewable energy efficiency and applicability on occasions where both heating and cooling are required simultaneously (e.g., buildings, agriculture). Therefore, in this study, we propose a new SHRC collector that consists of an upper transparent radiative emitter and a lower solar absorber and develop a mathematic model to numerically uncover the feasibility of realizing daytime SH and RC simultaneously.

2. Description of the SHRC module

The cross-section view of the SHRC module is shown in Fig. 1. A low-density polyethylene (PE) film, showing high transmissivity in the solar radiation band and far-infrared wavelength, is set at the top as the transparent cover. Separated by an air gap, a radiative emitter is positioned below the PE film. Another air cavity is arranged between the radiative emitter and an underneath solar absorber. To suppress thermal loss, a backside thermal insulation layer is placed at the bottom of the module. The radiative emitter and solar absorber are two key components of the SHRC module. The radiative emitter shows extremely high transmissivity in the solar radiation band and high emissivity in the "atmospheric window", while the solar absorber exhibits high absorptivity in the solar radiation band and low emissivity in the rest wavelengths. Fig. 2 illustrate the ideal spectral profile of the two surfaces. The extremely high solar transmissivity of the emitter allows the vast majority of incident solar radiation to penetrate the emitter and reach the absorber. This high solar transmissivity also means low absorptivity, preventing the emitter from heating by solar radiation. In addition, the high emissivity in the "atmospheric window" enables the emitter to strongly dissipate heat to the sky by

radiative cooling, and the low spectral emissivity (equals spectral absorptivity) in the rest bands allows the emitter to absorber the least radiative heat from surrounding warm bodies. For the absorber, its high solar absorptivity contributes to the capture of most incident solar radiation, while the low spectral absorptivity (equals spectral emissivity) restrains itself from significantly radiating heat to the sky and surrounding cold objects.

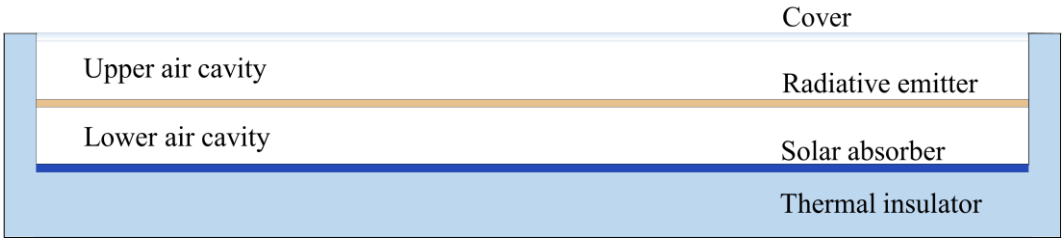

Fig. 1. The cross-section diagram of the SHRC module.

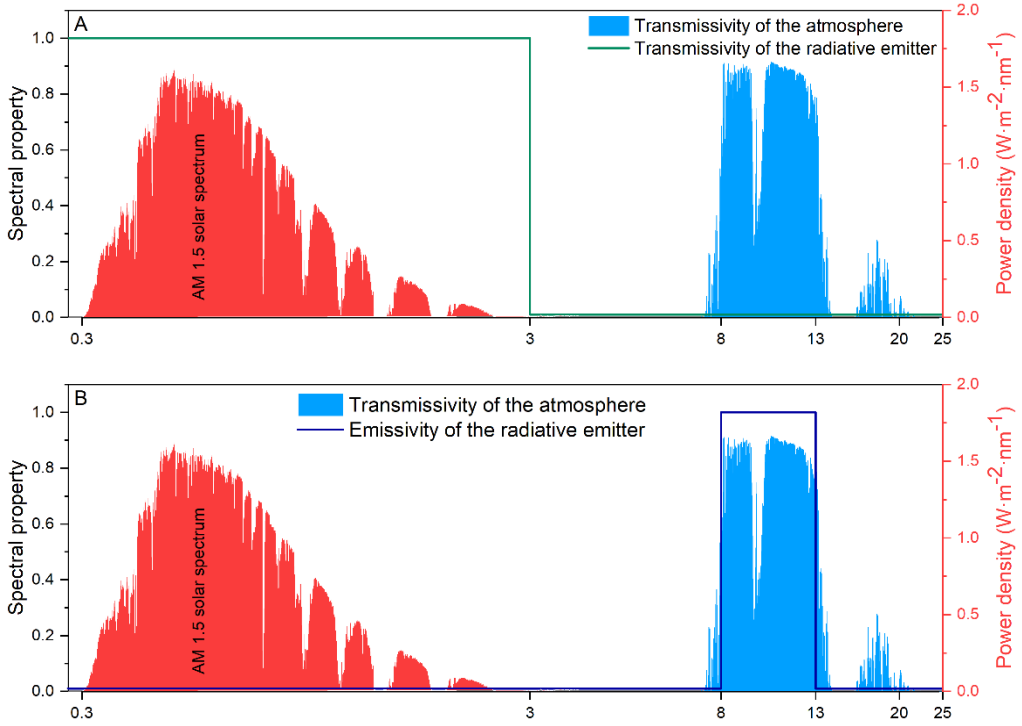

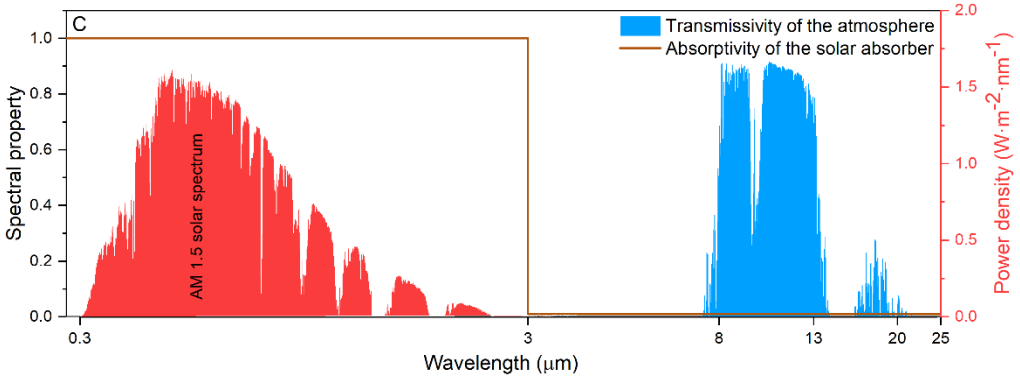

Fig. 2. Ideal spectral properties of the radiative emitter and solar absorber of the SHRC module. (A) Transmissivity of the emitter; (B) Emissivity of the emitter; (C) Absorptivity of the absorber. Note that an ideal emitter can show any transmissivity within 3–8 μm and above 13 μm.

3. Theoretical model

A theoretical model is developed in this section to characterize the thermal performance of the SHRC module. The model mainly includes three energy-balance equations, namely, the energy-balance equation for the transparent cover, the energy-balance equation for the radiative emitter, and the energy-balance equation for the solar absorber.

3.1. Energy-balance equation for the transparent cover

The energy-balance equation for the transparent cover is expressed as follows:

$$h_{ac}\left(T_a-T_c\right)+h_{ce}\left(T_e-T_c\right)+h_{sc}\left(T_s-T_c\right)+\alpha_c G=0 \quad (1)$$

where h_{ac} refers to the heat transfer coefficient between the ambient air and transparent cover, W/(m^2·K); h_{ce} is the heat transfer coefficient between the transparent cover and radiative emitter, W/(m^2·K); h_{sc} is the heat transfer coefficient between the sky and transparent cover, W/(m^2·K); T_a, T_c, and T_e are respectively the temperature of the ambient air, transparent cover, and radiative emitter, K; α_c is the effective solar absorptivity of the cover; and G is the solar irradiance, W/m^2.

The heat transfer coefficient between the ambient air and transparent cover is calculated by [28]:

$$h_{ac}=2.8+3.0u_a \quad (2)$$

where u_a is the ambient wind velocity, m/s.

The heat transfer coefficient between the transparent cover and radiative emitter consists of two parts, namely, the convective and radiative ones, and is written as:

$$h_{ce} = h_{ce\_conv} + h_{ce\_rad} = \frac{Nu \cdot k_a}{d_{ce}} + \frac{\sigma\left(T_c^2 + T_e^2\right)\left(T_c + T_e\right)}{1/\varepsilon_c + 1/\varepsilon_e - 1} \tag{3}$$

where Nu is the Nusselt number; k_a refers to the thermal conductivity of air, W/(m·K); d_{ce} denotes the air gap height between the cover and emitter, m; σ is the Stefan–Boltzmann constant, 5.67×10^{-8} $W/m^2 \cdot K^4$; and ε_c and ε_e are the total, hemispherical emissivity of the cover and emitter panel, respectively.

The heat transfer coefficient between the sky and cover is expressed as follows:

$$h_{sc} = \varepsilon_c \sigma \left(T_s^2 + T_c^2\right)\left(T_s + T_c\right) \tag{4}$$

The sky temperature is calculated by [29]:

$$T_s = 0.0552 T_a^{1.5} \tag{5}$$

3.2. Energy-balance equation for the radiative emitter

The energy-balance equation for the radiative emitter is written as follows:

$$h_{ce\_conv}\left(T_c - T_e\right) + h_{eab}\left(T_{ab} - T_e\right) + \alpha_e G + Q_{se} = 0 \tag{6}$$

where h_{eab} is the heat transfer coefficient between the emitter and absorber, $W/(m^2 \cdot K)$, and its expression is similar to that of the h_{ce}; T_{ab} means the absorber temperature, K; α_e is the effective solar absorptivity of the emitter; Q_{se} denotes the net radiative heat exchange between the sky and emitter, W/m^2, and is derived by [30]:

$$\begin{aligned} Q_{se} = Q_s - Q_e = & 2\int_0^{\infty}\int_0^{\pi/2} \varepsilon_s(\lambda,\theta)\cdot E_b(\lambda,T_a)\cdot \alpha_e(\lambda,\theta)\cdot \tau_c(\lambda,\theta)\sin\theta\cos\theta \mathrm{d}\theta \mathrm{d}\lambda \\ & - \int_0^{\infty}\left[\frac{E_b\left(\lambda,T_e\right)\cdot\left(1-\rho_{c,\lambda}\right) - \varepsilon_{c,\lambda}\cdot E_b\left(\lambda,T_c\right)}{1/\varepsilon_{e,\lambda} - \left(\left(1-\varepsilon_{e,\lambda}\right)/\varepsilon_{e,\lambda}\right)\cdot\rho_{c,\lambda}}\right]\mathrm{d}\lambda \end{aligned} \tag{7}$$

where Q_s refers to the absorbed radiant heat of the emitter from the sky, W/m^2; Q_e is the outward radiant heat from the emitter to the sky, which has included the radiative heat exchange between the emitter and cover, W/m^2; $\varepsilon_s(\lambda,\theta)$ denotes the spectral, directional emissivity of the sky; λ refers to the wavelength, μm; θ is the zenith angle, rad; $E_b(\lambda, T_a)$, $E_b(\lambda, T_e)$, and $E_b(\lambda, T_c)$ are respectively the spectral radiant power of the blackbody at ambient temperature, emitter temperature and cover temperature, W/(m^2·μm); $\alpha_e(\lambda,\theta)$ denotes the spectral, directional emissivity of the sky; $\tau_c(\lambda,\theta)$ is the spectral, directional transmissivity of the cover; $\rho_{c,\lambda}$ is the spectral reflectivity of the cover; $\varepsilon_{c,\lambda}$ denotes the spectral emissivity of the cover; and $\varepsilon_{e,\lambda}$ is the spectral emissivity of the emitter.

3.3. Energy-balance equation for the solar absorber

The energy-balance equation for the solar absorber is expressed as follows:

$$h_{eab}\left(T_e - T_{ab}\right) + h_{aab}\left(T_a - T_{ab}\right) + \alpha_{ab} G = 0 \tag{8}$$

where h_{aab} is the heat transfer coefficient between the ambient and absorber, W/(m^2·K), and is calculated by:

$$h_{aab} = \frac{1}{d_{th}/k_{th} + 1/h_{ath}} \tag{9}$$

where d_{th} and k_{th} respectively refer to the thickness and thermal conductivity of the thermal insulation layer, m and W/(m·K); and h_{ath} signifies the heat transfer coefficient between the ambient and insulation layer, which equals h_{ac} in formula, W/(m^2·K), and α_{ab} is the effective solar absorptivity of the absorber.

Detailed validation of the mathematic model can be found in Ref. [31].

4. Results and discussion

Based on the developed mathematic model, the thermal performance of the SHRC module is

analyzed in this section. It is quite clear that the solar absorber will be easily heated up to above-ambient temperatures when exposed to sunlight. What is not uncertain is that whether or not the radiative emitter can realize sub-ambient temperatures simultaneously. The key structural parameters of the SHRC module are set before the case study, as shown in Table 1. To realize daytime solar heating and radiative cooling simultaneously, the requirements for the spectral properties of the SHRC module is subtle. The transmissivity of the transparent cover should be as high as possible for both solar radiation and long-wave thermal emission, and the ideal spectral selectivity of the radiative emitter and solar absorber has been illustrated in Fig. 2. In this study, the benchmark spectral profiles of the cover [26], emitter [27], and absorber [32] are determined based on currently available materials which can meet the required spectral selectivity.

Table 1. Standard structure parameters of the SHRC module.

Components	Parameters	Values
Transparent cover	Length × width	0.5 × 0.5 m
	Emissivity (0.3–25 μm)	0.05
	Reflectivity (0.3–25 μm)	0.05
	Absorptivity (0.3–3 μm)	0.05
	Transmissivity (0.3–25 μm)	0.9
Radiative emitter	Length × width	0.5 × 0.5 m
	Emissivity and absorptivity (0.3–3 μm)	0.03
	Emissivity and absorptivity (8–13 μm)	0.95
	Emissivity and absorptivity (other bands)	0.05
	Transmissivity (0.3–3 μm)	0.9
Solar absorber	Length × width	0.5 × 0.5 m
	Emissivity and absorptivity (0.3–3 μm)	0.9
	Emissivity and absorptivity (3–25 μm)	0.05
Thermal insulation layer	Length × width × thickness	0.5 × 0.5 × 0.05 m
	Thermal conductivity	0.033 W/(m·K)
Air gap between the cover and emitter	Thickness	0.03 m
Air gap between the emitter and absorber	Thickness	0.03 m

4.1. Stagnation temperatures under different solar irradiances

First, the stagnation temperature of the radiative emitter and solar absorber under typical weather conditions is investigated. The ambient temperature, wind velocity and total water vapor

column is set at 25 °C, 2 m/s, and 300 atm-cm, respectively (the same for Sections 4.2 to 4.4). As shown in Fig. 3, the emitter and absorber temperatures increase with solar irradiance. When there is no solar radiation, namely, at night, the emitter can achieve a sub-ambient temperature (6.6 °C, non-vacuum case) easily. Under this condition, the absorber can also be cooled down by 14.5 °C due to heat exchange with the emitter. However, the emitter and absorber temperatures are very sensitive to solar irradiance. The absorber temperature lifts to above-ambient temperature even under extremely low solar intensities. Though with lower increasing rates, the emitter temperature also surges to above-ambient temperature once the solar irradiance exceeds 92 W/m^2. Even if the air cavity between the emitter and absorber is vacuumized to vanish the non-radiative heat transfer from the absorber to the emitter, the emitter is still unable to remain at a sub-ambient state if the solar irradiance is greater than 166 W/m^2. Therefore, although the solar absorptivity of the emitter is negligible, it cannot realize daytime radiative cooling in most cases due to significant heat absorption from the absorber. However, given that cold fluid such as water, air, or other coolants will take away the absorbed heat from the absorber and thus immensely decrease the absorber temperature in real-world solar thermal applications, the emitter might still be able to reach sub-ambient temperature under intense solar radiation. It is also worth pointing out that some little supports such as sticks may need to be added between the emitter and absorber to withstand the differential pressure between the upper and lower cavities if the latter is vacuumized.

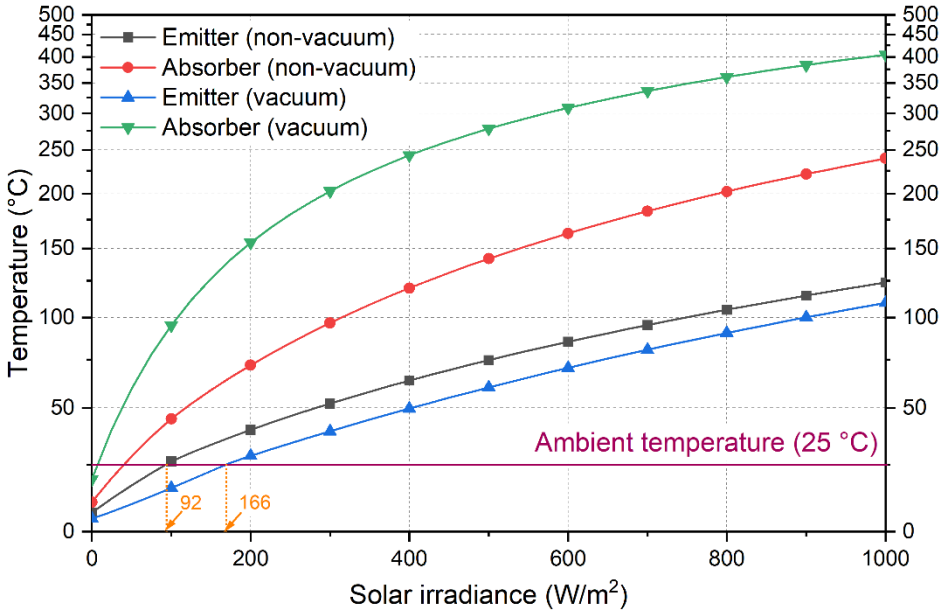

Fig. 3. The temperature of the emitter and absorber under different solar irradiances. The ambient temperature is set at 25 °C.

4.2. Effect of solar irradiance and absorber temperature

As discussed in section 4.1, the solar intensity and absorber temperature are two key factors determining the emitter temperature. Therefore, in this section, the coupling influence of solar irradiance and absorber temperature on the emitter temperature profile is evaluated. We assume that a hypothetical thermal carrier is introduced to adjust the absorber temperature varying between 25 and 70 °C. In this case, the energy-balance equation for the solar absorber (Eq. 8) is not involved in iteratively solving the energy-balance equation for the cover and emitter, for the absorber temperature has been given in advance. As shown in Fig. 4A, the emitter temperature shows a greater possibility of reaching sub-ambient radiative cooling as the thermal carrier suppresses the absorber temperature. In specific, if the absorber temperature is lower than 33.9 °C, the emitter can always cool itself to sub-ambient temperatures, even though the solar irradiance reaches 1000 W/m^2. However, once the absorber temperature exceeds 43.4 °C, the emitter temperature is always higher than the ambient temperature, even if there is no solar radiation. In this scenario, the emitter

temperature is dominated by the heat exchange between the emitter and absorber. Vacuumizing the air cavity between the two is an effective way to relieve the emitter from absorbing unwanted heat from the absorber, which is well-demonstrated in Fig. 4B. The emitter can realize a nearly 3 °C temperature reduction even under the given extremely harsh condition, namely, with an absorber temperature of 70 °C and solar irradiance of 1000 W/m^2. Fig. 4 also reveals that the emitter temperature is more sensitive to the absorber temperature for the non-vacuum case while more sensitive to the solar irradiance for the vacuum case. As the solar intensity is uncontrollable but the absorber temperature can be regulated manually, effectively extracting heat from the absorber by cold working mediums is critical to simultaneously realize daytime solar heating and radiative cooling, especially for the non-vacuum case which is more common and realistic.

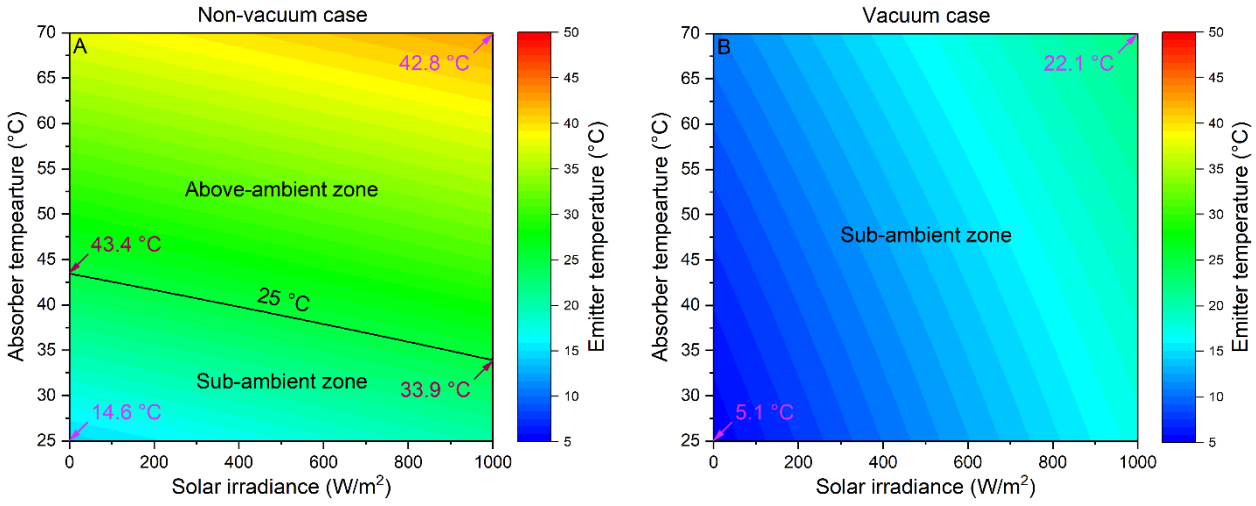

Fig. 4. Coupling effect of solar irradiance and absorber temperature on the emitter temperature profile in (A) Non-vacuum case and (B) Vacuum case. The ambient temperature is set at 25 °C.

4.3. Effect of solar irradiance and emitter solar-absorptivity

The solar absorptivity of the emitter is another important parameter that influences the emitter temperature. In general, the emitter should show as low as possible solar absorptivity but high enough solar transmissivity to enhance the daytime radiative cooling performance while ensuring

sufficient solar heating capacity. In this section, the coupling effect of solar irradiance and emitter solar-absorptivity on the emitter temperature profile in non-vacuum and vacuum cases with two absorber temperatures (i.e., 35 and 45 °C) is investigated. In this case study, the solar absorptivity is set less than 0.15 and the solar irradiance varies between 0 and 1000 W/m^2. As shown in Fig. 5A, the emitter can always realize sub-ambient radiative cooling if its solar absorptivity is less than 0.026 or the solar irradiance is lower than 201 W/m^2. For the vacuum case, however, the two values can be extended to 0.052 and 368 W/m^2. However, provided the absorber temperature increases to 45 °C, the emitter cannot cool itself to a sub-ambient state even if the solar absorptivity of the emitter is as low as 0.01 and the solar irradiance is zero, which further proves that the absorber temperature should be carefully regulated in the non-vacuum case. Once the vacuumization is involved, the absorber temperature is no longer a crucial factor for the realization of sub-ambient radiative cooling. Comparing Fig. 5C to Fig. 5B, it is clear that the thresholds of the emitter solar-absorptivity and solar irradiance for constant sub-ambient radiative cooling only decline by 21 W/m^2 and 0.003, respectively.

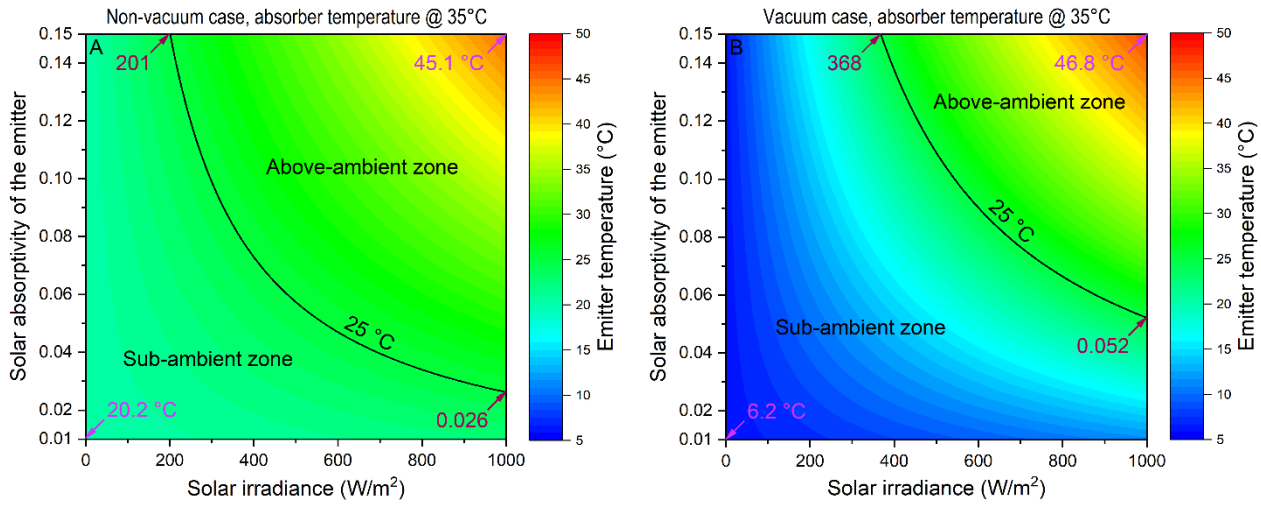

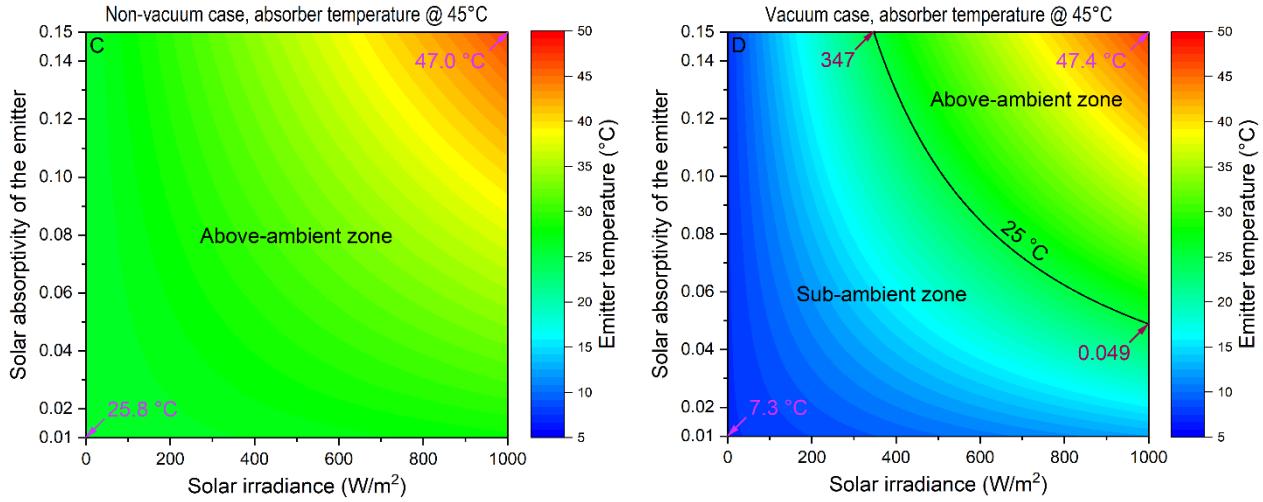

Fig. 5. Coupling effect of solar irradiance and solar absorptivity of the emitter on the emitter temperature profile in (A) Non-vacuum case with a constant absorber temperature of 35 °C, (B) Vacuum case with a constant absorber temperature of 35 °C, (C) Non-vacuum case with a constant absorber temperature of 45 °C, and (D) Vacuum case with a constant absorber temperature of 45 °C. The ambient temperature is set at 25°C.

4.4. Effect of solar irradiance and absorber emissivity

As previously discussed, the absorber plays a vital role in determining the emitter temperature in the non-vacuum case. Thus, the effect of the absorber emissivity on the emitter temperature profile is further assessed in this section. Higher absorber emissivity signifies greater radiative heat exchange between the emitter and absorber and thus higher emitter temperature, as shown in Fig. 6. However, the temperature gradient is very small with the change of absorber emissivity and solar intensity in the non-vacuum case. Specifically, the emitter temperature increases slowly from 20.2 to 27.9 °C as the absorber emissivity and solar irradiance shift from an extremely favorable situation (0.05 and 0 W/m^2) to an extremely unfavorable one (0.95 and 1000 W/m^2), indicating that the predominant heat input to the emitter is the non-radiative heat transferred from the absorber. This also could explain why the introduction of vacuumization in the air cavity between the emitter and absorber can improve the radiative cooling performance of the emitter as the non-radiative heat exchange (i.e., convective and conductive ones) will be eradicated. In the vacuum case, as shown in Fig. 6B, the emitter can always reach a sub-ambient temperature even though the absorber emitter

and solar irradiance are as high as 0.95 and 1000 W/m^2.

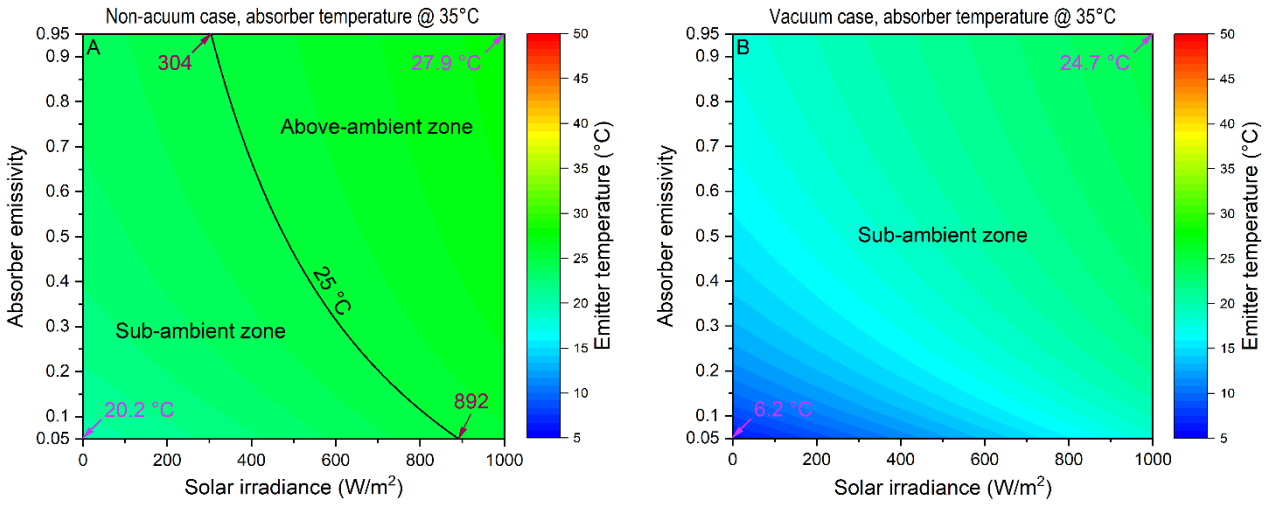

Fig. 6. Coupling effect of solar irradiance and absorber emissivity on the emitter temperature profile in (A) Non-vacuum case and (B) Vacuum case. The ambient and absorber temperatures are set at 25 and 35 °C, respectively.

4.5. Performance in three consecutive days

The thermal performance of the SHRC module in a consecutive 72 hours is further analyzed. The weather data from August 7th to 9th of the typical meteorological year in a subtropical city, Shanghai, is derived from the EnergyPlus Weather Data website [33] and employed for analysis in this study. We set the absorber temperature to be 10 °C higher than the ambient temperature throughout the 72 hours. As illustrated in Fig. 7, the emitter in both non-vacuum and vacuum cases can always cool itself to a sub-ambient temperature no matter on a clear day (August 7th) or mostly overcast day (August 8th) or cloudy day (August 9th). As expected, the emitter in the vacuum case shows much lower stagnation temperatures than in the non-vacuum case due to the eradication of non-radiative heat exchange between the emitter and absorber. During the nighttime, the emitter temperature is around 5 °C lower than the ambient temperature in the non-vacuum case and about 19 °C lower in the vacuum case. The temperature gap between the emitter and ambient air shrinks during the daytime, especially during peak sun hours. The minimum temperature reduction of the emitter is

only 0.8 °C for the non-vacuum case but still reaches 9.3 °C for the vacuum case.

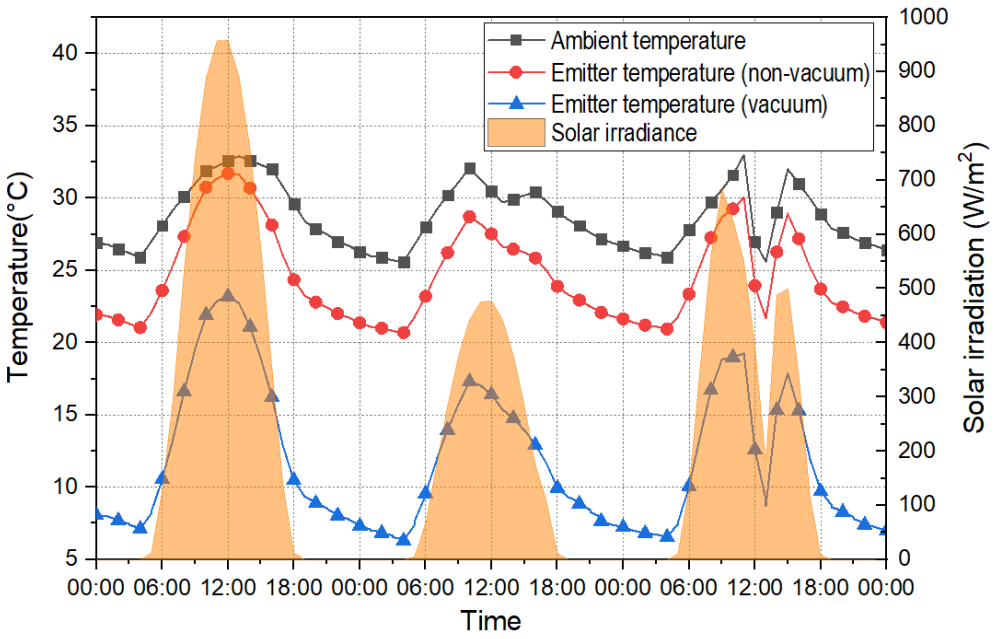

Fig. 7. The temperature variation of the emitter throughout three consecutive days in non-vacuum and vacuum cases. The weather data from August 7th to 9th of the typical meteorological year in Shanghai is employed for analysis.

5. Conclusions

In the present work, the possibility of realizing daytime solar heating (SH) and radiative cooling (RC) simultaneously using a single module is investigated. The novel SHRC module features an upper radiative emitter that shows extremely high solar transmissivity and a lower solar absorber with high solar absorptivity. The air cavity between the emitter and absorber can be vacuumized to achieve better cooling performance of the emitter. A mathematic model is developed to systematically analyze the thermal performance of the SHRC module under different working conditions. Simulation results demonstrate that the absorber temperature plays a vital role in determining the emitter temperature in the non-vacuum case. There is no way for the emitter to reach a sub-ambient temperature if the absorbed solar heat of the absorber cannot be effectively removed by thermal carriers, unless the solar irradiance is extremely low. However, as the absorber

temperature will remain only around 10 to 20 °C higher than the ambient temperature in real cases as the backside coolant, e.g., cold water flow, will promptly take away the absorber heat for other thermal utilizations, it is feasible to realize daytime SH and RC simultaneously for this module under certain cases. For example, with an ambient temperature of 25 °C, the emitter can always reach a sub-ambient temperature if the absorber temperature is lower than 33.9 °C in the non-vacuum case and can exceed 70 °C if the vacuumization is involved. The solar absorptivity of the emitter also significantly influences the emitter temperature during the daytime. This value should be as low as possible to assure the realization of sub-ambient radiative cooling even under intensive solar radiation. In contrast, the absorber emissivity is not that important to the successful completion of daytime sub-ambient radiative cooling, especially in the non-vacuum case, indicating that the predominant heat input to the emitter is the non-radiative heat transferred from the absorber. A three-consecutive-day thermal performance simulation for the SHRC module applied in a subtropical city, Shanghai, suggests that the emitter can always cool itself to a sub-ambient temperature under different weather conditions, with the minimum temperature reduction being 0.8 °C in the non-vacuum case and 9.3 °C in the vacuum case during peak sun hours.

Acknowledgments

This study was sponsored by the H2020 Marie Skłodowska-Curie Actions - Individual Fellowships (842096), National Natural Science Foundation of China (NSFC 51906241 and 51776193), and Anhui Provincial Natural Science Foundation (1908085ME138).

Nomenclature

d: thickness, m
E: radiant power, W/(m^2·μm)
G: solar irradiance, W/m^2

h: heat transfer coefficient, W/(m^2·K)
k: thermal conductivity, W/(m·K)
Nu: Nusselt number, -
Q: heat flux, W/m^2
T: temperature, K or °C
u: wind velocity, m/s
τ: transmittance, -
α: absorptivity, -
ε: emissivity, -
ρ: reflectivity, -
σ: Stefan–Boltzmann constant, 5.67×10^{-8} W/m$^2\cdot$K^4
λ: wavelength, μm
θ: zenith angle, rad

Abbreviation and subscripts
a: ambient
ab: solar absorber
b: blackbody
c: transparent cover
conv: convection
e: radiative emitter
th: thermal insulation layer
p: panel
rad: radiation
s: sky

References

[1] B. Dai, X. Zhao, S. Liu, Q. Yang, D. Zhong, Y. Cao, et al. Heating and cooling of residential annual application using DMS transcritical CO2 reversible system and traditional solutions: An environment and economic feasibility analysis. Energy Conversion and Management. 210 (2020) 112714.

[2] M.K. Nematchoua, M. Sadeghi, S. Reiter. Strategies and scenarios to reduce energy consumption and CO2 emission in the urban, rural and sustainable neighbourhoods. Sustainable Cities and Society. 72 (2021) 103053.

[3] Y. Tian, X. Liu, F. Chen, Y. Zheng. Harvesting energy from sun, outer space, and soil. Scientific reports. 10 (2020) 1-9.

[4] Y.-k. Chen, I.G. Jensen, J.G. Kirkerud, T.F. Bolkesjø. Impact of fossil-free decentralized heating on northern European renewable energy deployment and the power system. Energy. 219 (2021) 119576.

[5] D. Zhao, A. Aili, Y. Zhai, J. Lu, D. Kidd, G. Tan, et al. Subambient Cooling of Water: Toward Real-World Applications of Daytime Radiative Cooling. Joule. 3 (2019) 111-23.

[6] Y. Bie, M. Li, F. Chen, G. Królczyk, Z. Li. Heat transfer mathematical model for a novel parabolic trough solar collecting system with V-shaped cavity absorber. Sustainable Cities and Society. 52 (2020) 101837.

[7] G. Qiu, S. Yu, W. Cai. A novel heating strategy and its optimization of a solar heating system for a commercial building in term of economy. Energy. 221 (2021) 119773.

[8] B. Lamrani, F. Kuznik, A. Draoui. Thermal performance of a coupled solar parabolic trough collector latent heat storage unit for solar water heating in large buildings. Renewable Energy. 162 (2020) 411-26.

[9] A. Famiglietti, A. Lecuona, M. Ibarra, J. Roa. Turbo-assisted direct solar air heater for medium temperature industrial

processes using Linear Fresnel Collectors. Assessment on daily and yearly basis. Energy. 223 (2021) 120011.
[10] H. Ebrahimi, H. Samimi Akhijahani, P. Salami. Improving the thermal efficiency of a solar dryer using phase change materials at different position in the collector. Solar Energy. 220 (2021) 535-51.
[11] D. Zhao, A. Aili, Y. Zhai, S. Xu, G. Tan, X. Yin, et al. Radiative sky cooling: Fundamental principles, materials, and applications. Applied Physics Reviews. 6 (2019).
[12] M. Hu, Suhendri, B. Zhao, X. Ao, J. Cao, Q. Wang, et al. Effect of the spectrally selective features of the cover and emitter combination on radiative cooling performance. Energy and Built Environment. 2 (2021) 251-9.
[13] Y. Zhu, H. Qian, R. Yang, D. Zhao. Radiative sky cooling potential maps of China based on atmospheric spectral emissivity. Solar Energy. 218 (2021) 195-210.
[14] K. Zhang, D. Zhao, X. Yin, R. Yang, G. Tan. Energy saving and economic analysis of a new hybrid radiative cooling system for single-family houses in the USA. Applied Energy. 224 (2018) 371-81.
[15] J. Anand, D.J. Sailor, A. Baniassadi. The relative role of solar reflectance and thermal emittance for passive daytime radiative cooling technologies applied to rooftops. Sustainable Cities and Society. 65 (2021) 102612.
[16] R. Xiao, C. Hou, W. Yang, Y. Su, Y. Li, Q. Zhang, et al. Infrared-radiation-enhanced nanofiber membrane for sky radiative cooling of the human body. ACS applied materials & interfaces. 11 (2019) 44673-81.
[17] U. Eicker, A. Dalibard. Photovoltaic–thermal collectors for night radiative cooling of buildings. Solar Energy. 85 (2011) 1322-35.
[18] M. Farmahini Farahani, G. Heidarinejad, S. Delfani. A two-stage system of nocturnal radiative and indirect evaporative cooling for conditions in Tehran. Energy and Buildings. 42 (2010) 2131-8.
[19] A.P. Raman, M.A. Anoma, L. Zhu, E. Rephaeli, S. Fan. Passive radiative cooling below ambient air temperature under direct sunlight. Nature. 515 (2014) 540-4.
[20] B. Zhao, M. Hu, X. Ao, N. Chen, G. Pei. Radiative cooling: A review of fundamentals, materials, applications, and prospects. Applied Energy. 236 (2019) 489-513.
[21] L. Chen, K. Zhang, M. Ma, S. Tang, F. Li, X. Niu. Sub-ambient radiative cooling and its application in buildings. Building Simulation. Springer2020. pp. 1-25.
[22] M. Ono, K. Chen, W. Li, S. Fan. Self-adaptive radiative cooling based on phase change materials. Optics Express. 26 (2018) A777-A87.
[23] S. Taylor, L. Long, R. McBurney, P. Sabbaghi, J. Chao, L. Wang. Spectrally-selective vanadium dioxide based tunable metafilm emitter for dynamic radiative cooling. Solar Energy Materials and Solar Cells. 217 (2020) 110739.
[24] A. Ustaoglu, B. Kursuncu, M. Alptekin, M.S. Gok. Performance optimization and parametric evaluation of the cascade vapor compression refrigeration cycle using Taguchi and ANOVA methods. Applied Thermal Engineering. 180 (2020) 115816.
[25] M. Hu, B. Zhao, X. Ao, Y. Su, Y. Wang, G. Pei. Comparative analysis of different surfaces for integrated solar heating and radiative cooling: A numerical study. Energy. 155 (2018) 360-9.
[26] M. Hu, G. Pei, Q. Wang, J. Li, Y. Wang, J. Ji. Field test and preliminary analysis of a combined diurnal solar heating and nocturnal radiative cooling system. Applied Energy. 179 (2016) 899-908.
[27] Y. Zhai, Y. Ma, S.N. David, D. Zhao, R. Lou, G. Tan, et al. Scalable-manufactured randomized glass-polymer hybrid metamaterial for daytime radiative cooling. Science. 355 (2017) 1062-6.
[28] S. Li, Z. Chen, X. Liu, X. Zhang, Y. Zhou, W. Gu, et al. Numerical simulation of a novel pavement integrated photovoltaic thermal (PIPVT) module. Applied Energy. 283 (2021) 116287.
[29] A. Waqas, J. Ji. Thermal management of conventional PV panel using PCM with movable shutters – A numerical study. Solar Energy. 158 (2017) 797-807.
[30] M. Hu, B. Zhao, X. Ao, Suhendri, J. Cao, Q. Wang, et al. Performance analysis of a novel bifacial solar photothermic and radiative cooling module. Energy Conversion and Management. 236 (2021).

[31] M. Hu, B. Zhao, X. Ao, N. Chen, J. Cao, Q. Wang, et al. Feasibility research on a double-covered hybrid photo-thermal and radiative sky cooling module. Solar Energy. 197 (2020) 332-43.
[32] H. Wen, W. Wang, W. Wang, J. Su, T. Lei, C. Wang. Enhanced spectral absorption of bilayer WOx/SiO2 solar selective absorber coatings via low vacuum pre-annealing. Solar Energy Materials and Solar Cells. 202 (2019) 110152.
[33] EnergyPlus Weather Data (https://energyplus.net/weather).